arXiv:1901.11241v2 [cond-mat.mes-hall] 16 Jul 2020

Bulk-boundary correspondence for non-Hermitian Hamiltonians via Green functions

Heinrich-Gregor Zirnstein,[1] Gil Refael,[2] and Bernd Rosenow[1,3]

[1] *Institut für Theoretische Physik, Universität Leipzig, Brüderstrasse 16, 04103 Leipzig, Germany*
[2] *Institute of Quantum Information and Matter and Department of Physics, California Institute of Technology, Pasadena, CA 91125, USA*
[3] *Department of Condensed Matter Physics, Weizmann Institute of Science, Rehovot 76100, Israel*

(Dated: July 16, 2020)

Genuinely non-Hermitian topological phases can be realized in open systems with sufficiently strong gain and loss; in such phases, the Hamiltonian cannot be deformed into a gapped Hermitian Hamiltonian without energy bands touching each other. Comparing Green functions for periodic and open boundary conditions we find that, in general, there is no correspondence between topological invariants computed for periodic boundary conditions, and boundary eigenstates observed for open boundary conditions. Instead, we find that the non-Hermitian winding number in one dimension signals a topological phase transition in the bulk: It implies spatial growth of the bulk Green function.

Topology has made a profound impact on the description and design of wave-like systems such as quantum mechanical electrons [1–5] or light interacting with matter [6–11]. The key idea is to group physical systems, each described by a gapped (insulating) Hamiltonian, into the same topological class if their Hamiltonians can be continuously deformed into each other without closing the energy gap. For Hermitian Hamiltonians, the *bulk-boundary correspondence* states that topological invariants for periodic boundary conditions predict the presence of boundary states for open boundary conditions [1, 12–16].

Recently, non-Hermitian Hamiltonians [17–21] have attracted much attention; they describe open systems with loss (dissipation) and gain (e.g. coherent amplification in a laser) [22, 23]. Extending topological methods to these systems may be particularly beneficial for the design of topological protected laser modes [24–26]. Moreover, *genuinely non-Hermitian Hamiltonians*, i.e. Hamiltonians that cannot be deformed to a Hermitian Hamiltonian without energy bands touching, have novel topological properties not found in Hermitian systems. They can be characterized by topological invariants different from those of Hermitian systems [27–38], but the extent of a bulk-boundary correspondence is, surprisingly, much less clear [39–50].

We consider systems in one dimensions, which are particularly interesting because not only the eigenvectors but also the eigenenergies can have a nontrivial winding number. In the case of a two-band model with chiral symmetry, the Bloch Hamiltonian is off-diagonal

$$H(k) = \begin{pmatrix} 0 & q_+(k) \\ q_-(k) & 0 \end{pmatrix}. \tag{1}$$

In a lattice model, the lattice spacing forces the momentum k to be periodic, and the $q_\pm(k)$ describe closed paths in the complex plane. For example, a non-Hermitian Su-Schrieffer-Heeger (SSH) model is given by $q_\pm(k) = (m-1) + e^{\mp i(k - i\gamma)}$, and the paths are circles with different radii centered on the real axis. [51] The eigenvalues of the matrix $H(k)$ are distinct if neither path passes through the origin; in this case, we can assign to each path a winding number around the origin. These form the $\mathbb{Z}\times\mathbb{Z}$ topological invariant of a non-Hermitian Hamiltonian in symmetry class AIII [28]. Hermitian Hamiltonians are characterized by $q_+(k) = q_-(k)^*$, which forces both winding numbers to be opposites of each other; a single $\mathbb{Z}$-invariant remains [3, 52, 53]. Genuinely non-Hermitian phases appear whenever the two winding numbers are no longer opposites of each other [28, 33]. In this case, the *non-Hermitian winding number*, which is the winding number of the determinant $\det(H(k))$, is nonzero.

Is there a bulk-boundary correspondence for the non-Hermitian winding number? To answer this, we focus on response (Green) functions, which describe experimental observables for instance in a scattering setup. We find that the bulk-boundary correspondence breaks down once the non-Hermitian winding number takes a non-trivial value: When the winding number changes from zero, the bulk response starts exhibiting exponential *growth* in space, and since periodic systems cannot accommodate such spatial growth, they do not reflect the properties of systems with open boundaries. In this Letter, we focus on the specific example of non-Hermitian Dirac fermions to discuss the above physics, while a general proof is contained in the companion paper Ref. [54]. The growth of the bulk response is distinct from the so-called non-Hermitian skin effect [39, 41, 55–64].

Example: Dirac fermions with non-Hermitian terms.— We consider a continuum model that corresponds to the long distance limit of the non-Hermitian SSH model [32, 41, 65, 66]. It concerns wave functions with two components $\psi(x) = [\psi_1(x), \psi_2(x)]^T$ subject to

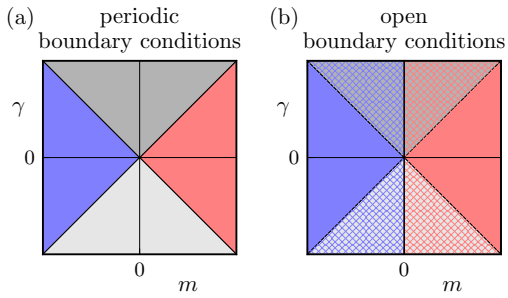


Figure 1. Topological phase diagram of one-dimensional non-Hermitian Dirac fermions with particle-hole symmetry and chiral symmetry. (a) Periodic boundary conditions. Two winding numbers distinguish four phases: Two Hermitian (red and blue) and two genuinely non-Hermitian phases (grey), separated by lines $\gamma = \pm m$. (b) Open boundary conditions. The line $m = 0$ separates phases with a different number of zero energy boundary eigenstates. For the boundary conditions (3), a positive mass implies the existence of a boundary state at each end (red), which are absent for a negative mass (blue). The lines $\gamma = \pm m$ now indicate that the bulk (and boundary) Green function change from exponential decay to exponential growth.

a Hermitian Dirac Hamiltonian $H_0 = m\sigma_x + (-i\partial_x)\sigma_y$, where σ_x, σ_y are Pauli matrices, m is a real mass parameter (band gap). Let us introduce non-Hermiticity by adding constant antihermitian terms:

$$\hat{H} = \hat{H}_0 + i\gamma\sigma_y, \tag{2}$$

where γ is real. There are three more terms that we could add: $i\gamma_x\sigma_x$, $i\gamma_z\sigma_z$, and $-i\Gamma\mathbb{1}$, where $\mathbb{1}$ is the identity matrix. The first can be absorbed by analytic continuation of the mass m. The second and third vanish if we also impose a chiral symmetry, $\{\hat{H}, \sigma_z\} = 0$, necessary for discussing zero energy boundary eigenstates in one dimension. Thus, the symmetry class is AIII [1] for complex m. For real mass m, $\hat{H}$ is additionally invariant under complex conjugation, placing it in symmetry class BDI, which also implies that eigenvalues occur in complex conjugate pairs.

In the continuum model (2), we have $q_\pm(k) = m \pm (\gamma - ik)$, and the paths described by $q_\pm(k)$ in the complex plane are no longer closed. Still, one can assign a half-integer winding number [33] that changes whenever a path crosses the origin. Such crossings happen at $\gamma = \pm m$ and we find the topological phase diagram in Fig. 1(a).

Open boundary conditions.— We now consider a system of length L with open boundary conditions

$$\psi_2(0) = 0, \ \psi_1(L) = 0 \tag{3}$$

corresponding to a particular boundary termination of the lattice model. For open boundary conditions, the non-Hermitian terms in both the Dirac-Hamiltonian Eq. (2) and the non-Hermitian SSH model defined below Eq. (1) can be eliminated by a similarity transformation: if $\psi_0(x)$ is an eigenfunction of the Hamiltonian $\hat{H}_0$, then $\psi(x) = e^{\gamma x}\psi_0(x)$ is an eigenfunction of the Hamiltonian $\hat{H}$. From this we see that *all* eigenfunctions are exponentially localized. This is the non-Hermitian skin effect [39, 41, 55–64].

Bulk and boundary Green function.— To clearly distinguish bulk and boundary, we now focus on Green functions, which are matrix-valued solutions to the equation

$$(E - \hat{H})G(E; x, y) = \mathbb{1}\delta(x - y) \ . \tag{4}$$

The *bulk Green function* G_{bulk} is defined as the response of an infinite system [54], whereas the Green function G_{open} for open boundary conditions is defined as the solution that satisfies the conditions (3). When we probe the system far away from the boundary, $0 \ll x, y \ll L$, then only the bulk of the system responds, and we expect that both Green functions give the same result. However, when the source is close to the boundary, $y \approx 0$ or $y \approx L$, we expect that reflection at the boundary is important, which is captured in the *boundary Green function*

$$G_{\text{bound}}(E; x, y) := G_{\text{open}}(E; x, y) - G_{\text{bulk}}(E; x - y). \tag{5}$$

It solves the homogeneous equation $(E - \hat{H})G_{\text{bound}}(E; x, y) = 0$. We have used that for a translationally invariant Hamiltonian, the bulk response only depends on the difference $x - y$. If G_0 denotes a Green function of $\hat{H}_0$ for open boundaries, then the corresponding retarded Green function for $\hat{H}$ reads

$$G(E; x, y) = G_0(E + i\eta; x, y)e^{\gamma(x-y)}, \tag{6}$$

with $\eta = 0^+$. We now focus on zero energy, $E = 0$. Then, we find

$$G_{0,\text{bulk}}(i\eta; x, y) = [\theta(-\tilde{x})G_L + \theta(\tilde{x})G_R]e^{-\sqrt{m^2+\eta^2}|\tilde{x}|}, \tag{7}$$

where $\tilde{x} = x - y$, and G_L and G_R are matrices

$$G_s = \mathcal{N}\begin{pmatrix} i\eta & m + \nu_s\sqrt{m^2+\eta^2} \\ m - \nu_s\sqrt{m^2+\eta^2} & i\eta \end{pmatrix} \tag{8}$$

with $s = L, R$, $\nu_{R/L} = \pm 1$, and $\mathcal{N} = 1/(2\sqrt{m^2+\eta^2})$. Thus, we obtain one of our main results: In the phases where the non-Hermitian winding number is nonzero, $|\gamma| > |m|$, the bulk Green function G_{bulk} grows exponentially as $x \to \pm\infty$ while keeping y fixed. For $G_{0,\text{bound}}$ near the left boundary, we find

$$G_{0,\text{bound}}(i\eta, x, y) = G_B e^{-\sqrt{m^2+\eta^2}(x+y)}, \text{ for } x, y \ll L. \tag{9}$$

Here, G_B is the matrix

$$G_B = -G_R \cdot \begin{pmatrix} \frac{m+\sqrt{m^2+\eta^2}}{m-\sqrt{m^2+\eta^2}} & 0 \\ 0 & 1 \end{pmatrix}. \tag{10}$$

Taken together, this yields the decomposition (5).

Boundary eigenstates.— The Green function can be expressed as a sum over eigenstates

$$G(E;x,y) = \sum_n (E-E_n)^{-1} \langle x|\psi_R^n\rangle\langle\psi_L^n|y\rangle. \tag{11}$$

Here, $|\psi_R^n\rangle$ are the so-called right- and $|\psi_L^n\rangle$ the left eigenstates of the non-Hermitian Hamiltonian, i.e. $H|\psi_R^n\rangle = E_n|\psi_R^n\rangle$ and $H^\dagger|\psi_L^n\rangle = E_n^*|\psi_L^n\rangle$ [67]. The contribution $\langle x|\psi_R^n\rangle\langle\psi_L^n|y\rangle$ of an individual eigenstate to the Green function can be extracted as the residue of the pole at $E = E_n$ [68, 69]. For identical positions $x = y$, this residue yields the biorthogonal polarization discussed in Ref. [40]. We now define a *boundary eigenstate* to be the residue of a pole of the *boundary* Green function, and focus on states at zero energy, $E = 0$. For open boundary conditions, our model has only real eigenvalues due to the relation Eq. (6), and we can obtain the residue from the imaginary part of the Green function since $\operatorname{Im} G(E+i0^+;x,y) = -\sum_n \langle x|\psi_R\rangle\langle\psi_L|y\rangle\delta(E-E_n)$ for real E. We find that

$$-\operatorname{Im} G^{11}{}_{\text{bound}}(0,x,y) = Ae^{(\gamma-m)x}e^{(-\gamma-m)y}, \quad \text{where } A = \theta(m)2m/\eta \text{ with } \eta = 0^+. \tag{12}$$

Thus, for $m > 0$, the boundary Green function has an isolated pole at zero energy, whose associated eigenstate is $\langle x|\psi_R^0\rangle = e^{(\gamma-m)x}$ and $\langle\psi_L^0|y\rangle = e^{(-\gamma-m)y}$. The spatial shape changes dramatically from exponentially localized to exponentially growing and vice versa whenever $\gamma = \pm m$. In contrast, for $m < 0$, no boundary eigenstate is found. Thus, the number of zero energy boundary eigenstates does not change during the topological phase transition at $\gamma = \pm|m|$ for periodic boundary conditions [Fig. 1(b)], and the bulk-boundary correspondence breaks down.

Bulk-periodic correspondence.— The traditional view on the bulk-boundary correspondence actually comprises two separate logical steps: it relates i) the bulk to the boundary Green function, and ii) the Green function G_{period} for periodic boundary conditions to that for the bulk of an infinite system: In the limit of large system size, both agree if the bulk Green function decays spatially [Fig. 2(a)]; this allows us to use topological invariants of the Bloch Hamiltonian (1) to characterize an infinite bulk. In non-Hermitian systems, step i) is unproblematic, but step ii) may fail. To better distinguish them, we propose to narrow the name *bulk-boundary correspondence* to refer only to the first step, and to call the second step the *bulk-periodic correspondence*.

Indeed, for our model in the regime $|\gamma| > |m|$, the bulk-periodic correspondence breaks down, because the periodic Green function decays, while the bulk Green function grows exponentially. [Fig. 2(b)] This growth also explains the exponential sensitivity to small perturbations seen in Ref. [44]. For periodic boundary conditions

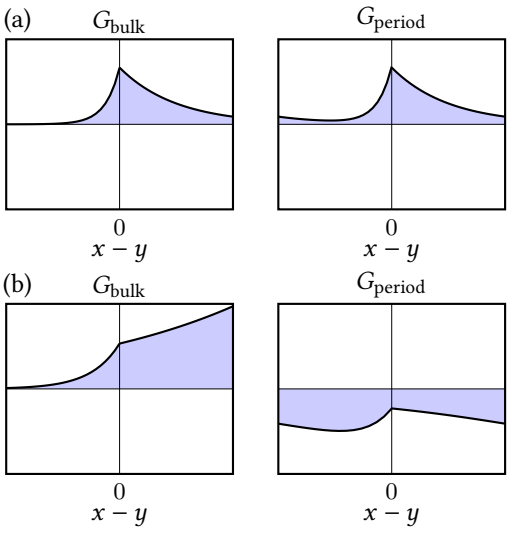


Figure 2. Breakdown of the bulk-periodic correspondence. (a) If the bulk Green function decays spatially, then both bulk and periodic Green function agree. (b) If the bulk Green function grows spatially, then the periodic Green function has to change drastically in order to accommodate periodic boundary conditions.

$\psi(-L/2) = \psi(+L/2)$, and using the results Eqs. (6) and (7) for the bulk Green function, we find

$$G_{\text{period}}(0;x,0) = G_{\text{bulk}}(0;x,0) + G_L\frac{e^{\kappa_L x}}{e^{\kappa_L L}-1} + G_R\frac{e^{\kappa_R x}}{e^{-\kappa_R L}-1}. \tag{13}$$

with $\kappa_{L/R} = \gamma \pm \sqrt{m^2+\eta^2}$. In the limit of large system size, $L \gg |x|$, the two additional terms vanish if only if the exponents satisfy $\kappa_L > 0$ and $\kappa_R < 0$, i.e. if the bulk Green function decays spatially [Fig. 2].

If we focus on bulk growth and disregard boundary eigenstates, we no longer require symmetry class AIII. Then, we find our main result, which holds both with and without symmetry (class A): If the non-Hermitian winding number is nonzero, then the bulk Green function at zero energy grows spatially. For example, consider a general Dirac model $\hat{H} = (-i\partial_x)\tau_1 + m_1\tau_1 + m_2\tau_2 + \cdots + m_n\tau_n - i\Gamma\mathbb{1}$ where the τ_j are Hermitian gamma matrices, $\{\tau_i,\tau_j\} = 2\delta_{ij}$, the masses m_j are complex and $\Gamma \geq 0$. Then, since $(\hat{H}+i\Gamma)^2$ is proportional to the identity matrix, the corresponding bulk Green function has form $G_{\text{bulk}}(0;x,0) = G_L\theta(-x)e^{\kappa_L x} + G_R\theta(x)e^{\kappa_R x}$ with $\kappa_{L,R} = -im_1 \pm \sqrt{m_2^2+\cdots+m_n^2+\Gamma^2}$ and appropriate $G_{L,R}$. Here, the branch of the complex square root is the one with positive real part; we choose it by demanding that we remain in the same branch when $\Gamma \to \infty$ [54]. Thus, the Green function grows in space if and only if the imaginary part of m_1 exceeds the real part of the root. Imposing symmetries will only constrain the parameters, but not affect this conclusion. In general, the Green func-

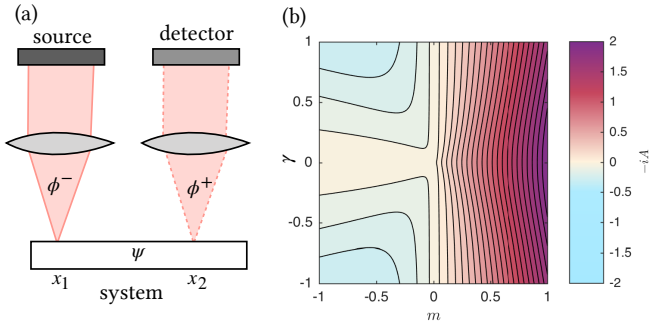


Figure 3. (a) Scattering setup. (b) Scattering response of the one-dimensional Dirac fermion with dissipation $\Gamma = |\gamma|$. The plot shows the amplitude $-iA$ of the boundary response at the left boundary.

tion is a sum of exponentials $\exp(ik_s x)$ where the complex momenta k_s are the zeros of $\det(H(k))$; the subscript s refers to a side L, R and an index. For local continuum models like the Dirac model, this determinant is a polynomial in momentum k. Thus, the non-Hermitian winding number $\nu(H) = (2\pi)^{-1} \int_{-\infty}^{\infty} dk\, \partial_k \arg\det(H(k))$ is the sum of $+1/2$ for each zero above the real axis and $-1/2$ for each zero below. But this number changes precisely when one of the zeros crosses the real axis, which means that the exponential changes from spatial decay to spatial growth. We extend this sketch to a full proof for lattice models in Ref. [54]. While for the above Dirac models, exponential growth only occurs in the genuinely non-Hermitian phases, for other models, it may arise even when the Hamiltonian can be deformed to a Hermitian one; see [51] for an example. Thus, the growth of the bulk Green function is not, by itself, topologically invariant.

Our work still leaves open the exciting question of the bulk-boundary correspondence in the narrow sense: Are there topological invariants of the bulk Green function that imply the presence of boundary eigenstates? For Dirac fermions, the latter persist well into the genuinely non-Hermitian phases. This is also true for lattice models discussed in the literature [32, 39–42, 44], see the Supplemental Material [51] for details.

Experimental response: Scattering.— In a scattering configuration [see Fig. 3(a)], an excitation of an outside field ϕ is created, and the incoming amplitude ϕ^- targets a point x_1 of the system. If the excitation is monochromatic with frequency (energy) E, then the system will eventually reach a stationary state ψ that, in turn, emits an outgoing amplitude ϕ^+ at every position x_2. The scattering matrix $S(E)$ records how incoming amplitudes are mapped to outgoing amplitudes, $\phi^+ = S(E)\phi^-$, and is given by the Mahaux-Weidenmüller formula [70]

$$S(E) = \mathbb{1} - 2iW^\dagger \frac{1}{E - \hat{H}} W, \quad \hat{H} = \hat{H}_0 - iWW^\dagger \quad (14)$$

Here, the matrix W describes how the outside field couples into the system. The Hamiltonian $\hat{H}_0$ describes the time evolution of the system if the coupling was absent; it is usually Hermitian, for it is the combination with the dissipative term $-iWW^\dagger$ that yields an effective non-Hermitian Hamiltonian $\hat{H}$. The scattering matrix differs from unity by $-2iW^\dagger G(E)W$ where $G(E)$ is the Green function of this non-Hermitian Hamiltonian. To make this Letter self-contained, in the Supplemental Material [51] we include an elementary discussion of the Mahaux-Weidenmüller formula [71, 72], which is equivalent to *temporal coupled mode-theory* [73, 74] in optics.

So far, we have shown how coupling to an environment yields a non-Hermitian Hamiltonian. Conversely, we now consider a Hamiltonian H and attempt to realize it in a scattering setup. For this, we decompose it as $\hat{H} = \hat{H}_0 + i\hat{\Gamma}$ where $\hat{H}_0 = [\hat{H} + \hat{H}^\dagger]/2$ and $\hat{\Gamma} = (i/2)[\hat{H}^\dagger - \hat{H}]$ are Hermitian matrices. We define a Hamiltonian to be *purely dissipative* if $\hat{\Gamma}$ is negative semidefinite, $\hat{\Gamma} \leq 0$, i.e. if it has no positive eigenvalues. Any matrix of the form $\hat{\Gamma} = -WW^\dagger$ is negative semidefinite, and any semidefinite $\hat{\Gamma}$ can be represented in the above form by choosing $W = (-\hat{\Gamma})^{1/2}$. This choice is unique up to a change of basis for the outside field, $W \to WU$, with U unitary, and up to components that do not couple. Thus, any purely dissipative Hamiltonian can be realized in a scattering setup described by Eq. (14). But in order to realize a general non-Hermitian Hamiltonian, we have to allow for positive eigenvalues in the antihermitian part, which corresponds to (linear) *gain*, i.e. coherent amplification. In fact, gain is a key requirement for the non-Hermitian winding number to be nonzero, see Ref. [54].

In optical systems, gain can be realized by optical pumping [75], and spatially uniform gain can be described by the ansatz $\hat{H} = \hat{H}_0 + ig - iWW^\dagger$ with a positive constant g in Eq. (14). Then, the antihermitian part of $\hat{H}$ is related to the coupling matrix via $-WW^\dagger = \hat{\Gamma} - g$, and this relation can be solved for W if the non-Hermitian Hamiltonian $\hat{H}$ has *bounded gain*, i.e. if $\hat{\Gamma} - g$ becomes negative semidefinite by making g sufficiently large. For example, the Dirac fermion, Eq. (2), can be described by $\hat{H} = \hat{H}_0 + ig - iWW^\dagger$ with $g = |\gamma|$, $W = \sqrt{|\gamma|}[1, -\mathrm{sgn}(\gamma)i]^T$; the coupling W is a 2×1 matrix when modeling the outside field as a scalar.

Since a purely dissipative setup can be realized more easily than one with gain, we ask whether signatures of the zero energy boundary states of the Dirac fermion Eq. (2) can still be found without gain. This corresponds to allowing a constant dissipation, $\hat{H} = \hat{H}_0 + i\gamma\sigma_y - i\Gamma\mathbb{1}$, which does break chiral symmetry. We consider the special case $\Gamma = |\gamma|$, which has the least amount of dissipation while probing the phase transition region $\gamma = \pm|m|$.

At zero energy, we can use Eq. (9) with $\eta = \Gamma$ and find

$$[W^\dagger G_{\text{bound}}(E=0)W](x_2, x_1 = 0) = A \exp\left(-x_2/\xi_L\right),$$
$$A = -i\frac{m}{\sqrt{m^2+\gamma^2}}\frac{\gamma^2}{m-\sqrt{m^2+\gamma^2}}, \qquad (15)$$

where A denotes the amplitude and $\xi_L = 1/(\sqrt{m^2+\gamma^2}-\gamma)$ the localization length of the response. We see that the amplitude can still distinguish the phase with boundary eigenstate, $m > 0$, from the phase without, $m < 0$, though the distinction is less sharp [Fig. 3(b)] than in the case with gain and chiral symmetry.

Conclusion.— Using the example of non-Hermitian Dirac fermions, we have discussed the topological phase diagram via Green functions. The key idea was to decompose the Green function for open boundary conditions into a bulk and a boundary Green function, Eq. (5). We have shown that a nonzero non-Hermitian winding number means that the correspondence of the open system to a periodic one breaks down due to an exponential growth of the bulk Green function. We have also discussed how to realize non-Hermitian Hamiltonian in a scattering setup and indicated that observing a nonzero topological invariant requires a system with gain.

Acknowledgements.— We would like to thank T. Karzig for helpful discussions. B. R. and H.-G. Z. acknowledge financial support from the German Research Foundation within the Collaborative Research Centre 762 (project B6). B. R. acknowledges support from the Rosi and Max Varon Visiting Professorship at the Weizmann Institute of Science. We are grateful for the hospitality of the Aspen Center for Physics, funded by NSF grant PHY-1607611, where part of this work was performed. G. R. is grateful for generous support from the Institute of Quantum Information and Matter, an NSF frontier center, NSF grant 1839271, and The Simons Foundation.

[1] M Zahid Hasan and C L Kane, "Colloquium: Topological insulators," Rev. Mod. Phys. **82**, 3045–3067 (2010).
[2] Xiao-Liang Qi and Shou-Cheng Zhang, "Topological insulators and superconductors," Rev. Mod. Phys. **83**, 1057–1110 (2011).
[3] Ching-Kai Chiu, Jeffrey C Y Teo, Andreas P Schnyder, and Shinsei Ryu, "Classification of topological quantum matter with symmetries," Rev. Mod. Phys. **88**, 035005 (2016), arXiv:1505.03535v2.
[4] B Andrei Bernevig and Taylor L Hughes, *Topological Insulators and Topological Superconductors* (Princeton University Press, 2013).
[5] A Bansil, Hsin Lin, and Tanmoy Das, "Colloquium: Topological band theory," Rev. Mod. Phys. **88**, 021004 (2016).
[6] S Raghu and F D M Haldane, "Analogs of quantum-Hall-effect edge states in photonic crystals," Phys. Rev. A **78**, 033834 (2008).
[7] Ling Lu, John D. Joannopoulos, and Marin Soljačić, "Topological photonics," Nat. Photonics **8**, 821–829 (2014).
[8] Alexander B Khanikaev and Gennady Shvets, "Two-dimensional topological photonics," Nat. Photonics **11**, 763–773 (2017).
[9] Mikael C. Rechtsman, Julia M. Zeuner, Yonatan Plotnik, Yaakov Lumer, Daniel Podolsky, Felix Dreisow, Stefan Nolte, Mordechai Segev, and Alexander Szameit, "Photonic Floquet topological insulators," Nature **496**, 196–200 (2013).
[10] Yonatan Plotnik, Mikael C. Rechtsman, Daohong Song, Matthias Heinrich, Julia M. Zeuner, Stefan Nolte, Yaakov Lumer, Natalia Malkova, Jingjun Xu, Alexander Szameit, Zhigang Chen, and Mordechai Segev, "Observation of unconventional edge states in 'photonic graphene'," Nat. Mater. **13**, 57–62 (2014).
[11] Jiho Noh, Wladimir A. Benalcazar, Sheng Huang, Matthew J. Collins, Kevin P. Chen, Taylor L. Hughes, and Mikael C. Rechtsman, "Topological protection of photonic mid-gap defect modes," Nat. Photonics **12**, 408 (2018).
[12] B. I. Halperin, "Quantized Hall conductance, current-carrying edge states, and the existence of extended states in a two-dimensional disordered potential," Phys. Rev. B **25**, 2185–2190 (1982).
[13] Yasuhiro Hatsugai, "Chern number and edge states in the integer quantum Hall effect," Phys. Rev. Lett. **71**, 3697–3700 (1993).
[14] Andrew M. Essin and Victor Gurarie, "Bulk-boundary correspondence of topological insulators from their respective Green's functions," Phys. Rev. B **84**, 125132 (2011).
[15] Gian Michele Graf and Marcello Porta, "Bulk-Edge Correspondence for Two-Dimensional Topological Insulators," Commun. Math. Phys. **324**, 851–895 (2013).
[16] Julio Cesar Avila, Hermann Schulz-Baldes, and Carlos Villegas-Blas, "Topological Invariants of Edge States for Periodic Two-Dimensional Models," Math Phys Anal Geom **16**, 137–170 (2013).
[17] Naomichi Hatano and David R. Nelson, "Localization Transitions in Non-Hermitian Quantum Mechanics," Phys. Rev. Lett. **77**, 570–573 (1996).
[18] Carl M Bender and Stefan Boettcher, "Real Spectra in Non-Hermitian Hamiltonians Having PT Symmetry," Phys. Rev. Lett. **80**, 5243–5246 (1998).
[19] Ingrid Rotter, "A non-Hermitian Hamilton operator and the physics of open quantum systems," J. Phys. Math. Theor. **42**, 153001 (2009).
[20] Hui Cao and Jan Wiersig, "Dielectric microcavities: Model systems for wave chaos and non-Hermitian physics," Rev. Mod. Phys. **87**, 61–111 (2015).
[21] Bo Zhen, Chia Wei Hsu, Yuichi Igarashi, Ling Lu, Ido Kaminer, Adi Pick, Song-Liang Chua, John D Joannopoulos, and Marin Soljačic, "Spawning rings of exceptional points out of Dirac cones," Nature **525**, 354–358 (2015).
[22] Stefano Longhi, "Parity-time symmetry meets photonics: A new twist in non-Hermitian optics," EPL **120**, 64001 (2017).
[23] Ramy El-Ganainy, Konstantinos G. Makris, Mercedeh Khajavikhan, Ziad H. Musslimani, Stefan Rotter, and Demetrios N. Christodoulides, "Non-Hermitian physics and PT symmetry," Nat. Phys. **14**, 11–19 (2018).

[24] Babak Bahari, Abdoulaye Ndao, Felipe Vallini, Abdelkrim El Amili, Yeshaiahu Fainman, and Boubacar Kanté, "Nonreciprocal lasing in topological cavities of arbitrary geometries," Science **358**, 636 (2017).

[25] P. St-Jean, V. Goblot, E. Galopin, A. Lemaître, T. Ozawa, L. Le Gratiet, I. Sagnes, J. Bloch, and A. Amo, "Lasing in topological edge states of a one-dimensional lattice," Nat. Photonics **11**, 651 (2017).

[26] Midya Parto, Steffen Wittek, Hossein Hodaei, Gal Harari, Miguel A. Bandres, Jinhan Ren, Mikael C. Rechtsman, Mordechai Segev, Demetrios N. Christodoulides, and Mercedeh Khajavikhan, "Edge-Mode Lasing in 1D Topological Active Arrays," Phys. Rev. Lett. **120**, 113901 (2018).

[27] Emil J. Bergholtz, Jan Carl Budich, and Flore K. Kunst, "Exceptional Topology of Non-Hermitian Systems," arXiv:1912.10048 (2019), arXiv:1912.10048.

[28] Zongping Gong, Yuto Ashida, Kohei Kawabata, Kazuaki Takasan, Sho Higashikawa, and Masahito Ueda, "Topological phases of non-Hermitian systems," Phys. Rev. X **8**, 031079 (2018), arXiv:1802.07964.

[29] Kohei Kawabata, Ken Shiozaki, Masahito Ueda, and Masatoshi Sato, "Symmetry and Topology in Non-Hermitian Physics," Phys. Rev. X **9**, 041015 (2019).

[30] Hengyun Zhou and Jong Yeon Lee, "Periodic table for topological bands with non-Hermitian symmetries," Phys. Rev. B **99**, 235112 (2019), arXiv:1812.10490.

[31] Nadav M. Shnerb and David R. Nelson, "Winding Numbers, Complex Currents, and Non-Hermitian Localization," Phys. Rev. Lett. **80**, 5172–5175 (1998).

[32] Tony E Lee, "Anomalous Edge State in a Non-Hermitian Lattice," Phys. Rev. Lett. **116**, 133903 (2016).

[33] Daniel Leykam, Konstantin Y Bliokh, Chunli Huang, Y D Chong, and Franco Nori, "Edge Modes, Degeneracies, and Topological Numbers in Non-Hermitian Systems," Phys. Rev. Lett. **118**, 040401 (2017).

[34] Huitao Shen, Bo Zhen, and Liang Fu, "Topological Band Theory for Non-Hermitian Hamiltonians," Phys. Rev. Lett. **120**, 146402 (2018).

[35] Simon Lieu, "Topological symmetry classes for non-Hermitian models and connections to the bosonic Bogoliubov–de Gennes equation," Phys. Rev. B **98**, 115135 (2018).

[36] Mark R. Hirsbrunner, Timothy M. Philip, and Matthew J. Gilbert, "Topology and observables of the non-Hermitian Chern insulator," Phys. Rev. B **100**, 081104(R) (2019), arXiv:1901.09961.

[37] S. Longhi, "Topological Phase Transition in non-Hermitian Quasicrystals," Phys. Rev. Lett. **122**, 237601 (2019), arXiv:1905.09460.

[38] Yu Chen and Hui Zhai, "Hall conductance of a non-Hermitian Chern insulator," Phys. Rev. B **98**, 245130 (2018).

[39] Ye Xiong, "Why does bulk boundary correspondence fail in some non-hermitian topological models," J. Phys. Commun. **2**, 035043 (2018).

[40] Flore K Kunst, Elisabet Edvardsson, Jan Carl Budich, and Emil J Bergholtz, "Biorthogonal Bulk-Boundary Correspondence in Non-Hermitian Systems," Phys. Rev. Lett. **121**, 026808 (2018).

[41] Shunyu Yao and Zhong Wang, "Edge States and Topological Invariants of Non-Hermitian Systems," Phys. Rev. Lett. **121**, 086803 (2018).

[42] Ching Hua Lee and Ronny Thomale, "Anatomy of skin modes and topology in non-Hermitian systems," Phys. Rev. B **99**, 201103(R) (2019).

[43] L. Jin and Z. Song, "Bulk-boundary correspondence in a non-Hermitian system in one dimension with chiral inversion symmetry," Phys. Rev. B **99**, 081103(R) (2019), arXiv:1809.03139.

[44] Loïc Herviou, Jens H. Bardarson, and Nicolas Regnault, "Defining a bulk-edge correspondence for non-Hermitian Hamiltonians via singular-value decomposition," Phys. Rev. A **99**, 052118 (2019).

[45] Zi-Yong Ge, Yu-Ran Zhang, Tao Liu, Si-Wen Li, Heng Fan, and Franco Nori, "Topological band theory for non-Hermitian systems from the Dirac equation," Phys. Rev. B **100**, 054105 (2019).

[46] Dan S. Borgnia, Alex Jura Kruchkov, and Robert-Jan Slager, "Non-Hermitian Boundary Modes and Topology," Phys. Rev. Lett. **124**, 056802 (2020), arXiv:1902.07217.

[47] Wojciech Brzezicki and Timo Hyart, "Hidden Chern number in one-dimensional non-Hermitian chiral-symmetric systems," Phys. Rev. B **100**, 161105(R) (2019).

[48] Kazuki Yokomizo and Shuichi Murakami, "Non-Bloch Band Theory of Non-Hermitian Systems," Phys. Rev. Lett. **123**, 066404 (2019).

[49] Kohei Kawabata, Nobuyuki Okuma, and Masatoshi Sato, "Non-Bloch band theory of non-Hermitian Hamiltonians in the symplectic class," Phys. Rev. B **101**, 195147 (2020), arXiv:2003.07597.

[50] Zhesen Yang, Kai Zhang, Chen Fang, and Jiangping Hu, "Auxiliary generalized Brillouin zone method in non-Hermitian band theory," arXiv:1912.05499 (2019), arXiv:1912.05499.

[51] See Supplemental Material at ... for non-Hermitian extensions of the SSH lattice model and an elementary discussion of the Mahaux-Weidenmüller formula.

[52] Andreas P Schnyder, Shinsei Ryu, Akira Furusaki, and Andreas W W Ludwig, "Classification of topological insulators and superconductors in three spatial dimensions," Phys. Rev. B **78**, 195125 (2008).

[53] Alexei Kitaev, "Periodic table for topological insulators and superconductors," in *AIP Conf. Proc.* (2009) p. 22.

[54] Heinrich-Gregor Zirnstein and Bernd Rosenow, "Exponentially growing bulk Green functions as signature of nontrivial non-Hermitian winding number in one dimension," arXiv:2007.07026 (2020), arXiv:2007.07026.

[55] V. M. Martinez Alvarez, J. E. Barrios Vargas, and L. E. F. Foa Torres, "Non-Hermitian robust edge states in one dimension: Anomalous localization and eigenspace condensation at exceptional points," Phys. Rev. B **97**, 121401(R) (2018).

[56] V. M. Martinez Alvarez, J. E. Barrios Vargas, M. Berdakin, and L. E. F. Foa Torres, "Topological states of non-Hermitian systems," Eur. Phys. J. Spec. Top. (2018), 10.1140/epjst/e2018-800091-5.

[57] Kai Zhang, Zhesen Yang, and Chen Fang, "Correspondence between winding numbers and skin modes in non-hermitian systems," arXiv:1910.01131 (2020), arXiv:1910.01131.

[58] Nobuyuki Okuma, Kohei Kawabata, Ken Shiozaki, and Masatoshi Sato, "Topological Origin of Non-Hermitian Skin Effects," Phys. Rev. Lett. **124**, 086801 (2020), arXiv:1910.02878.

[59] Nobuyuki Okuma and Masatoshi Sato, "Hermitian zero modes protected by nonnormality: Application

of pseudospectra," Phys. Rev. B **102**, 014203 (2020), arXiv:2005.01704.

[60] Lei Xiao, Tianshu Deng, Kunkun Wang, Gaoyan Zhu, Zhong Wang, Wei Yi, and Peng Xue, "Non-Hermitian bulk–boundary correspondence in quantum dynamics," Nat. Phys. (2020), 10.1038/s41567-020-0836-6, arXiv:1907.12566.

[61] T. Helbig, T. Hofmann, S. Imhof, M. Abdelghany, T. Kiessling, L. W. Molenkamp, C. H. Lee, A. Szameit, M. Greiter, and R. Thomale, "Generalized bulk–boundary correspondence in non-Hermitian topolectrical circuits," Nat. Phys. , 1–4 (2020), arXiv:1907.11562.

[62] Tobias Hofmann, Tobias Helbig, Frank Schindler, Nora Salgo, Marta Brzezińska, Martin Greiter, Tobias Kiessling, David Wolf, Achim Vollhardt, Anton Kabaši, Ching Hua Lee, Ante Bilušić, Ronny Thomale, and Titus Neupert, "Reciprocal skin effect and its realization in a topolectrical circuit," Phys. Rev. Research **2**, 023265 (2020), arXiv:1908.02759.

[63] Tsuneya Yoshida, Tomonari Mizoguchi, and Yasuhiro Hatsugai, "Mirror skin effect and its electric circuit simulation," Phys. Rev. Research **2**, 022062 (2020), arXiv:1912.12022.

[64] Stefano Longhi, "Probing non-Hermitian skin effect and non-Bloch phase transitions," Phys. Rev. Research **1**, 023013 (2019).

[65] Simon Lieu, "Topological phases in the non-Hermitian Su-Schrieffer-Heeger model," Phys. Rev. B **97**, 045106 (2018).

[66] Kenta Esaki, Masatoshi Sato, Kazuki Hasebe, and Mahito Kohmoto, "Edge states and topological phases in non-Hermitian systems," Phys. Rev. B **84**, 205128 (2011).

[67] Dorje C Brody, "Biorthogonal quantum mechanics," J. Phys. Math. Theor. **47**, 035305 (2014).

[68] R E Peierls, "Complex Eigenvalues in Scattering Theory," Proc. R. Soc. Math. Phys. Eng. Sci. **253**, 16–36 (1959).

[69] Maciej Zworski, "Resonances in physics and geometry," Not. Am. Math. Soc. **46**, 319–328 (1999).

[70] Claude Mahaux and Hans A Weidenmüller, *Shell-Model Approach to Nuclear Reactions* (North-Holland Pub. Co., 1969).

[71] Mikhail S Livsic, *Operators, Oscillations, Waves. (Open Systems)* (American Mathematical Society, 1973).

[72] Y V Fyodorov and H J Sommers, "Spectra of Random Contractions and Scattering Theory for Discrete-Time Systems," J. Exp. Theor. Phys. Lett. **72**, 422–426 (2000).

[73] Wonjoo Suh, Zheng Wang, and Shanhui Fan, "Temporal coupled-mode theory and the presence of non-orthogonal modes in lossless multimode cavities," IEEE J. Quantum Electron. **40**, 1511–1518 (2004).

[74] Shanhui Fan, Wonjoo Suh, and J D Joannopoulos, "Temporal coupled-mode theory for the Fano resonance in optical resonators," Opt. Soc. Am. J. **20**, 569–572 (2003).

[75] Exponential amplification cannot be indefinite; in practice, gain will saturate nonlinearly [76].

[76] Simon Malzard, Emiliano Cancellieri, and Henning Schomerus, "Topological dynamics and excitations in lasers and condensates with saturable gain or loss," Opt. Express **26**, 22506 (2018), arXiv:1705.06895.

Supplemental Material: Bulk-boundary correspondence for non-Hermitian Hamiltonians via Green functions

Heinrich-Gregor Zirnstein, Gil Refael, and Bernd Rosenow

Lattice models

In this section, we present the topological phase diagrams for periodic and open boundary conditions for several lattice models with chiral symmetry, and discuss the spatial growth of their bulk Green function.

A non-Hermitian extension of the Su-Schrieffer-Heeger (SSH) model is given by Eq. (1) with

$$q_\pm(k) = (m-1) + e^{\mp i(k - i\gamma)}. \tag{16}$$

The paths $q_\pm(k)$ in the complex plane are circles with center $(m-1)$ and radius $e^{\mp\gamma}$. They wind around the origin whenever the radius exceeds the distance of the center from the origin. For open boundary condition, the model can be mapped to the Hermitian SSH Hamiltonian $\tilde{H} = S^{-1}HS$ with the same mass parameter by the similarity transform $(S\psi)_j = e^{j\gamma}\psi_j$ where ψ_j denotes the wave function at site j. Thus, the presence or absence of boundary eigenstates at zero energy is determined solely by m. The topological phase diagram is shown in Fig. 4(a).

In the literature, a different non-Hermitian extension of the SSH model has been discussed [32, 39–42, 44]. It is given by Eq. (1) with

$$q_\pm(k) = (m-1) \pm \gamma/2 + e^{\mp ik}. \tag{17}$$

The paths are circles with unit radius, but their center is shifted by a distance $\gamma/2$ along the real axis. For open boundary conditions, the model can be mapped to a Hamiltonian $\tilde{H} = S^{-1}HS$ with off-diagonal entries

$$\tilde{q}_\pm(k) = \sqrt{(m-1)^2 - (\gamma/2)^2} + e^{\mp ik}. \tag{18}$$

This Hamiltonian is Hermitian if $|m-1| > |\gamma/2|$; this region includes the point $(m,\gamma) = (0,0)$ that features prominently in the continuum model. Here, the similarity transform is given by $(S\psi)_j = r^j \,\mathrm{diag}(1,r)\psi_j$ where diag denotes a 2×2-diagonal matrix and $r = \sqrt{[(m-1)-\gamma/2]/[(m-1)+\gamma/2]}$ [41]. Thus, the boundary eigenstates eigenstates at zero energy are determined by a Hermitian SSH model with different parameters. For the region where this transformation does not yield a Hermitian Hamiltonian, we refer to Ref. [41]. The phases are shown in Fig. 4(b).

We have indicated that if the non-Hermitian winding number is nonzero, then the bulk Green function grows exponentially. For lattice models, this can be justified as follows: If the model has short-range hopping, then the Hamiltonian is a (Laurent) polynomial $H(k) = \tilde{H}(z)$ in the variables $z = e^{ik}$ and $z^{-1} = e^{-ik}$. In the generic case, the bulk Green function can be written as a sum of exponentials z_s^j, where j denotes a lattice site, and the z_s are the complex zeros of $\det \tilde{H}(z)$. Each zero inside the unit circle contributes $+1$, while each zero outside the unit circle contributes -1 to the non-Hermitian winding number $\nu(H) = (2\pi)^{-1}\int_0^{2\pi} dk\, \partial_k \arg\det(H(k))$. (There are also contributions from a pole at $z=0$.) Thus, the winding number changes when one of the zeros crosses the unit circle, i.e. when $|z_s| < 1$ changes to $|z_s| > 1$, or vice versa; this means a change in spatial growth. We refer to the companion paper Ref. [54] for a full proof. That said, if two zeros cross the unit circle simultaneously, then it is possible that no change in spatial growth occurs; this happens, for example, when the sign of the mass is changed in the Hermitian SSH model.

The converse statement is not true: It may happen that the non-Hermitian winding number is zero, but the bulk Green function grows exponentially. This occurs for

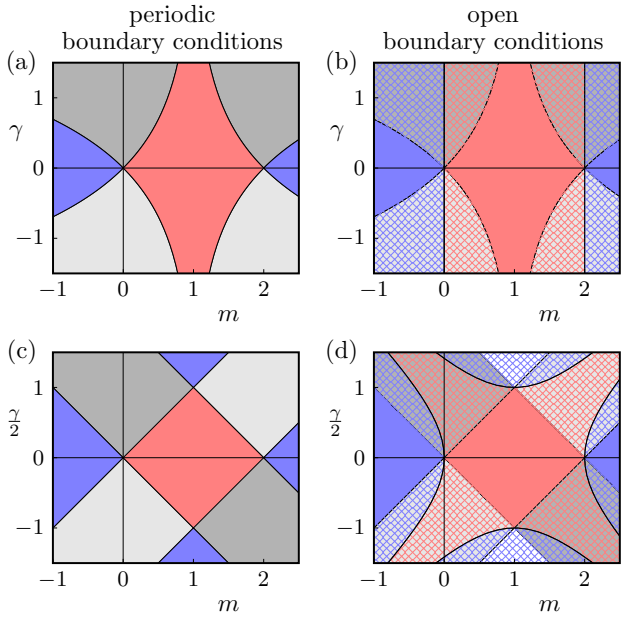


Figure 4. Topological phases of non-Hermitian SSH models. For periodic boundary conditions, (a) and (c), solid colors distinguish four different combinations of the two winding numbers. Different grey tones represent different non-Hermitian phases, where the bulk Green function grows spatially. For open boundary conditions, (b) and (d), red (blue) indicates the presence (absence) of boundary eigenstates at zero energy. Around the point $(m,\gamma) = (0,0)$, both diagrams agree with the phase diagram of the continuum model from the main text [Fig. 1]. (a-b) Lattice model Eq. (16). (c-d) Lattice model Eq. (17).

the model (17) in the parameter region $|\gamma/2| > |m-1|+1$ [Fig 4(c-d)]. If we allow the parameter m to become complex, thus leaving the BDI symmetry class while remaining in AIII, spatial growth may happen even when the Bloch Hamiltonian can be deformed to a Hermitian Bloch Hamiltonian without crossing zero energy. Setting $m = 1+te^{i\phi}$ where $t > 0$ and ϕ is real, we find, for $\gamma = 0$,

$$q_\pm(k) = te^{i\phi} + e^{\mp ik}. \tag{19}$$

Changing ϕ continuously deforms the corresponding Hamiltonian; for $\phi = 0$, the Hamiltonian is Hermitian and the bulk Green function decays in space, while for $\phi = \pi/2$, the Hamiltonian is non-Hermitian and features gain $+it$. It is plausible that if $t \gg 1$, then the bulk Green function grows exponentially. In more detail, the zeros of $\det\left(\tilde{H}(z) - i\Gamma\right)$ are

$$z_{1,2}(i\Gamma) = \frac{i}{2}\left[\frac{1+\Gamma^2-t^2}{t} \pm \sqrt{\frac{(1+\Gamma^2-t^2)^2}{t^2}+4}\right], \tag{20}$$

where $\Gamma > 0$ denotes an additional dissipation. During analytic continuation from $\Gamma = +\infty$ to $\Gamma = 0$, both zeros cross the unit circle if and only if $t > 1$, which means that the bulk Green function grows exponentially in this parameter regime [54].

Phenomenological justification of the Mahaux-Weidenmüller formula

In this section, we present a phenomenological justification of the Mahaux-Weidenmüller formula, Eq. (14), for the scattering setup illustrated in Fig. 3(a) of the main text.

The Mahaux-Weidenmüller formula calculates the scattering matrix of a system, which describes how a monochromatic incoming amplitude ϕ^- at energy E is mapped to an outgoing amplitude $\phi^+ = S(E)\phi^-$. We repeat it here for convenience:

$$S(E) = \mathbb{1} - 2iW^\dagger \frac{1}{E - \hat{H}_0 + iWW^\dagger} W. \tag{21}$$

The system is described by the Hamiltonian $\hat{H}_0$, while the matrix W maps the outside field to a state inside the system, and vice versa for $W^\dagger$. Here, the matrix products are to be understood as integrals over space and sums over internal degrees of freedom. For example, $W\phi^- \equiv \sum_\sigma \int dx_1\, W_{\tau\sigma}(x, x_1)\phi^-_\sigma(x_1)$, where x_1, x denote positions, and τ, σ internal degrees of freedom.

The formula can be justified by the following ansatz: [72–74] Let us denote the state of the internal system by ψ. If the system were isolated, then this state would evolve according to the linear Schrödinger equation $i\partial_t\psi = \hat{H}_0\psi$. If the Hamiltonian $\hat{H}_0$ is Hermitian, then the square integral of the state is conserved, $\partial_t(\psi^\dagger\psi) = 0$; this corresponds to the conservation of probability in quantum mechanics, or energy in optics. To couple the system to the outside field, we now make a linear ansatz

$$i\partial_t\psi = A\psi + B\phi^- \tag{22a}$$
$$\phi^+ = C\psi + D\phi^-, \tag{22b}$$

with some matrices A, B, C, D, which we assume to be constant in time. The conservation law now becomes

$$\partial_t(\psi^\dagger\psi) = (\phi^-)^\dagger\phi^- - (\phi^+)^\dagger(\phi^+), \tag{23}$$

which means that the incoming and outgoing amplitudes may add to or remove from the conserved quantity of the system state. In optics, this ansatz is known as temporal coupled-mode theory [73, 74]. After some algebra, we obtain that the combination of the ansatz and the conservation law is equivalent to the equations

$$i\partial_t\psi = \hat{H}_0\psi - \frac{1}{\sqrt{2}}W(\phi^+ + S_0\phi^-) \tag{24a}$$
$$(\phi^+ - S_0\phi^-) = i\sqrt{2}W^\dagger\psi, \tag{24b}$$

and the constraints that $\hat{H}_0$ be Hermitian and S_0 be unitary. The first equation can be viewed as a Schrödinger equation with a source term, and the second as a constraint that relates the outside field and the system. We proceed by making a change of basis for $S_0\phi^- \to \phi^-$, so that we can assume that S_0 is the identity matrix. Then, we make the ansatz of a harmonic motion $\psi(t) = e^{-iEt}\psi(E)$ and eliminate ψ from the equations and the Mahaux-Weidenmüller formula follows.

The ansatz is phenomenological. In real systems, the coupling W may be energy-dependent, and instead of focusing the outside field to a single point x_1, one may have to consider plane waves incident at different angles. We present a more microscopic derivation in the next section.

Microscopic derivation of the Mahaux-Weidenmüller formula

In this section, we present a self-contained derivation of the Mahaux-Weidenmüller formula, Eq. (14), for a microscopic model of the scattering setup illustrated in Fig. 3(a) of the main text. In the setup, we label the horizontal direction by x and the vertical direction by z.

For simplicity, we will model the outside field as a scalar field $\phi(t, x, z)$ that propagates according to the wave equation, $(\partial_t^2 - \Delta)\phi = 0$. A monochromatic configuration with energy E that satisfies the wave equation can be expanded in terms of ingoing amplitudes ϕ^+_α and

outgoing amplitudes ϕ_α^-:

$$\phi_E(t,x,z) = e^{-iEt}\left[\sum_\alpha \left[\phi_\alpha^+ e^{ik_z^\alpha z} + \phi_\alpha^- e^{-ik_z^\alpha z}\right] u_\alpha(x) + \sum_\beta \phi_\beta^+ e^{-\kappa^\beta z} u_\beta(x)\right]. \quad (25)$$

Here, the functions $u_\alpha(x)$ are eigenfunctions of the one-dimensional Laplacian, $u_\alpha(x) \propto \exp(ik_x^\alpha x)$ where α labels the possible horizontal momenta k_x^α. When this momentum is not too large, the field can propagate in z-direction with wave vector $k_z^\alpha = \sqrt{E^2 - (k_x^\alpha)^2}$. This is known as an open scattering channel. On the other hand, if the horizontal momentum is larger than the available energy, the scattering channel is closed, and only an evanescent wave with decay $\kappa_z^\beta = \sqrt{(k_x^\alpha)^2 - E^2}$ remains. For notational clarity, we reserve the label β for this case.

The scattering problem now asks to calculate the outgoing amplitudes ϕ_α^+ from the incoming amplitudes ϕ_α^-. The solution is the scattering matrix $S(E)$, which gives $\phi_+^\alpha = \sum_{\alpha\tilde{\alpha}} S_{\alpha\tilde{\alpha}}(E)\phi_{\tilde{\alpha}}^-$.

To do that, we need to specify the dynamics of the internal system and the coupling to the outside. We have already indicated that internal system is located at $z = 0$, and its state represented by a function $\psi(t,x)$ that evolves according to a Schrödinger equation $i\partial_t\psi = \hat{H}_0\psi$ with a Hermitian Hamiltonian $\hat{H}_0$. The most economic way to specify the whole setup is to write a Lagrangian $L = L_\phi + L_\psi + L_V$ with terms

$$L_\phi = \frac{1}{2}\int dx \int_0^\infty dz\,[(\partial_t\phi^*)(\partial_t\phi) - (\nabla\phi^*)\cdot(\nabla\phi)] \quad (26a)$$

$$L_\psi = \int dx\,\psi^\dagger(t,x)(i\partial_t - \hat{H}_0)\psi(t,x) \quad (26b)$$

$$L_V = \psi^\dagger V\phi|_{z=0} + \phi^*|_{z=0}V^\dagger\psi. \quad (26c)$$

The first terms gives the wave equation, the second term the Schrödinger equation, and the third term is a potential energy that couples the outside field at the boundary $z = 0$ to the internal state via an operator V. We proceed by deriving the equations of motion while paying special attention to the boundary terms at $z = 0$, and find

$$i\partial_t\psi = \hat{H}_0\psi - V\phi|_{z=0} \quad (27a)$$

$$\partial_z\phi|_{z=0} = -2V^\dagger\psi. \quad (27b)$$

In other words, the values $\phi|_{z=0}$ of the outside field at the boundary act as a source term for the Schrödinger equation, while the internal state poses a constraint on the spatial derivative $\partial_z\phi|_{z=0}$ of the outside field. For a harmonic oscillation, $i\partial_t \to E$, we can solve the equations of motion and obtain the scattering matrix

$$S_{\alpha\tilde{\alpha}}(E) = \delta_{\alpha\tilde{\alpha}} - \sum_{i,j}\frac{4i}{k_z^\alpha}(V^+)_{\alpha i}\left[\frac{1}{E - H_{\text{eff}}}\right]_{ij} V_{j\tilde{\alpha}}, \quad (28)$$

where i,j label orthonormal states of the state ψ, and

$$H_{\text{eff},ij} = \hat{H}_{0,ij} - \sum_\beta \frac{2}{\kappa^\beta}V_{i\beta}(V^+)_{\beta j} - i\sum_\alpha \frac{2}{k_z^\alpha}V_{i\alpha}(V^+)_{\alpha j} \quad (29)$$

is an effective Hamiltonian. It contains both additional Hermitian terms that arise from the closed scattering channels, and additional antihermitian terms that arise from the open scattering channels. To obtain the Mahaux-Weidenmüller formula in the phenomenological form presented in the main text, we have to perform several simplifications: (a) the Hermitian Hamiltonian $\hat{H}_0$ is redefined to incorporate the potential energy due to the closed channels, (b) the matrix $W_{i\alpha}$ is obtained from $V_{i\alpha}$ by normalizing the scattering amplitudes with $\sqrt{k_z^\alpha}$, (c) the energy dependence of k_z^α is neglected, making $W_{i\alpha}$ independent of energy, and (d) transforming the Fourier basis $u_\alpha(x)$ back to the position basis, if desired.